Journal of Power Sources 213 (2012) 40–46

Contents lists available at SciVerse ScienceDirect

Journal of Power Sources

journal homepage: www.elsevier.com/locate/jpowsour

# Nonlinear viscoelastic–plastic constitutive description of proton exchange membrane under immersed condition

Shouwen Shi [a], Dunji Yu [a], Lilan Gao [a], Gang Chen [a], Jian Chen [b], Xu Chen [a,*]

[a] School of Chemical Engineering and Technology, Tianjin University, 92 Weijin Road, Nankai District, Tianjin 300072, China

[b] Key Laboratory of Efficient & Clean Energy Utilization, College of Hunan Province, University of Science and Technology, Changsha 410114, China

ARTICLE INFO

*Article history:*
Received 29 December 2011
Received in revised form
18 March 2012
Accepted 19 March 2012
Available online 21 April 2012

*Keywords:*
Nonlinear viscoelastic
Water immersion
Nafion
plastic deformation
Constitutive law

ABSTRACT

The nonlinear viscoelastic–plastic responses of proton exchange membrane (PEM) under immersed condition at 30 and 70 °C are experimentally studied. For the description of the viscoelastic–plastic behavior of the material, Schapery's nonlinear viscoelastic model is used in combination with a nonlinear viscoplastic constitutive law. PEM's creep–relaxation behavior is predicted by the model with a constant duration at various stresses and a fixed stress level with different durations. The prediction results are found to agree quite well with experimental values at 30 °C. A step-stress input profile is conducted to validate the model and the result shows reasonable agreement with the experimental data indicating that the proposed model provides the capability to describe the characteristic of membranes in liquid water. However, this model cannot describe the creep behavior at 70 °C precisely mainly due to the distinct behavior of the membrane at the temperature. Thus, a modified model is developed and prediction values of the modified model at 30 and 70 °C are both found to be in good accordance with experimental results.



## 1. Introduction

Proton exchange membranes (PEMs) are commonly utilized in a growing number of applications including fuel cells, batteries, and solar cells due to their advantages in terms of high proton conductivity, good chemical stability, and mechanical integrity [1]. However, one of the barriers inhibiting the widespread commercialization of this technology is the limitation of the lifetime under operating conditions [2–4] which is believed to be the contribution of prolonged build-up of stresses of the constrained membranes resulted from the hygrothermal cycles in fuel cell environment [5]. In particular, compressive stresses resulted from swelling of the membrane and tensile residual stresses driven from shrinkage of the membrane lead to the failure of the membrane [2]. A better understanding of the mechanical behaviors of the membranes subjected to hygrothermal cycles will be helpful for developing life prediction models to estimate durability and improve operation. The mechanical responses of PEM subjected to a wide range of relative humidity and temperature levels have received considerable attention by many researchers and are available in literatures [1,2,6–11].

To better understand hydration effects on durability, characterization of PEMs under liquid water saturation as an extreme exposure condition is necessary, as the membrane may experience contact with liquid water during operation. The effects of water on membranes have been a subject of focus and intensively studied by many researchers [1,6,7,9,12]. Majsztrik et al. [9] recently reported the temperature-dependent of viscoelastic response of Nafion subjected to various humidity levels. They showed that water acted to plasticize Nafion at $T < 40$ °C while stiffen it at $T > 90$ °C which was also observed by Bauer et al. [13]. Silberstein and Boyce [6] studied the biomaterial swelling conditions in conjunction with modeling, examining the effect of loading via constrained swelling. An interesting phenomenon was observed by Kusoglu et al. [1] via investigating the mechanical properties and swelling behaviors of the membranes in liquid water, they found that when Nafion was submerged in water it was more appropriate to model it as a rubber rather than as a semicrystalline polymer. The constitutive response of ionomer membranes over a range of humidity and temperature levels including liquid water were investigated by Yoon and Huang [7]. The Schroeder's paradox referring to the phenomena that the water uptake of a membrane in saturated water vapor differ from that in liquid water at the same temperature, is a subject of debate and has been investigated by many researchers both from microscopic and macroscopic views [14–19].

* Corresponding author. Tel.: +86 22 27408399; fax+86 22 27403389.
*E-mail address:* xchen@tju.edu.cn (X. Chen).

0378-7753/$ – see front matter © 2012 Elsevier B.V. All rights reserved.
doi:10.1016/j.jpowsour.2012.03.082

Despite the growing number of literature on the role of water plays in the membrane, appropriate constitutive models to accurately predict the stresses that develop in operating fuel cells are rarely reported. Thus, the intent of this study is to find an appropriate model to capture the distinctive mechanical properties of PEMs under immersed condition. In this study, a viscoelastic–plastic model as a function of stress and time based on the method proposed by Lou and Schapery [20] is used and then validated. Besides, this model is also modified for better description of the creep-recovery behavior of the membrane, especially at 70 °C.

## 2. Experiments

Commercially available Nafion®-212 membranes developed and manufactured by DuPont with the thickness of 50 μm were used in this study. Specimens were cut into stripes with the length of 15 mm and width of 6 mm using a template and a scalpel. Prior to testing, theses samples were immersed in deionized (DI) water for 24 h in the thermostat water bath (HSY-2MB) as pretreatment to make them fully hydrated. The creep tests were carried out on Dynamic Mechanical Analysis (DMA-Q800, TA instruments) with film submersion clamp as shown in Fig. 1. The fluid tank in Fig. 1(b) was saturated with water to ensure that membrane samples were fully hydrated all the time during the experiments. In addition, experiments were carried out wearing disposable gloves to avoid any contamination of the membranes.

In order to validate the stress-dependence of the membrane and at the same time to determine the onset of the nonlinearity, creep-recovery tests were conducted at various stress levels, such as 1, 2, 4, 5 as well as 6 MPa, with the duration of 30 min followed by recovery duration of 1 h to make the specimens fully recovered as much as possible. Hence, the remaining strains measured at the end of the tests were treated as viscoplastic strain. In addition, so as to determine the viscoplastic strain parameters, another two sets of creep-recovery experiments were carried out at a fixed stress level of 5 MPa with the duration of 20 min and 50 min followed by recovery duration of 40 min and 90 min, respectively, as shown in Table 1. To validate the model, a step-stress profile was conducted, and prediction from the model was matched against the experimental data. All the experiments mentioned above were conducted at 30 °C in liquid water.

At 70 °C, similar experiments as that at 30 °C were conducted on the membranes in liquid water as shown in Table 1. Since the temperature tested was much higher than the ambient temperature in the room, in order to eliminate the effect of temperature, water in the fluid tank was preheated to 70 °C and then the membrane was transferred immediately from the thermostat that was also 70 °C to the submersion clamp.

**Table 1**
Creep–recovery experiments.

| Temperature (°C) | Stress (MPa) | Duration (min) | |
|---|---|---|---|
| | | Creep | Recovery |
| 30 | 1 | 30 | 60 |
| 30 | 2 | 30 | 60 |
| 30 | 4 | 30 | 60 |
| 30 | 5 | 20 | 40 |
| 30 | 5 | 30 | 60 |
| 30 | 5 | 50 | 90 |
| 30 | 6 | 30 | 60 |
| 70 | 1 | 30 | 60 |
| 70 | 2 | 30 | 60 |
| 70 | 3 | 20 | 40 |
| 70 | 3 | 30 | 60 |
| 70 | 3 | 50 | 100 |

## 3. Constitutive model

A general nonlinear constitutive theory for multiaxial loading was proposed by Schapery, from which, as a very special case, a simple stress–strain equation was derived for uniaxial loading [20]. The constitutive equation for uniaxial loading is given by

$$\varepsilon(t) = g_0 D_0 \sigma + g_1 \int_0^t \Delta D(\psi - \psi') \frac{dg_2\sigma}{d\tau} d\tau + \varepsilon_{vp} \quad (1)$$

where $D_0$ and $\Delta D(\psi)$ are the initial and transient components of the linear viscoelastic creep compliance, respectively. In addition, $\varepsilon$ and $\sigma$ are creep strain and stress applied on the membrane, respectively, and $\varepsilon_{vp}$ represents the viscoplastic strain generated during loading. Also, the reduced time

$$\psi = \psi(t) = \int_0^\tau \frac{dt'}{a_\sigma} \text{ and } \psi' = \psi(\tau) = \int_0^t \frac{dt'}{a_\sigma} \quad (2)$$

and $g_0$, $g_1$, $g_2$ and $a_\sigma$ are stress-dependent properties which also have thermodynamic origin. Particularly, changes in $g_0$, $g_1$ and $g_2$ are the inflection of third and higher order stress-dependence of the Gibbs free energy [21]. In general, $a_\sigma$ known as the shift factor, may depend on stress and temperature, as well as humidity. In this study, however, with the environment kept fixed in the tests, the shift factor $a_\sigma$ will become a function of stress only. When the applied stress is sufficiently low, $g_0 = g_1 = g_2 = a_\sigma = 1$, hence, Eq. (1) reduces to the familiar Boltzmann superposition integral for linear viscoelastic behavior in Eq. (3)

$$\varepsilon(t) = D_0 \sigma + \int_0^t \Delta D(t - \tau) \frac{d\sigma}{d\tau} d\tau + \varepsilon_{vp} \quad (3)$$

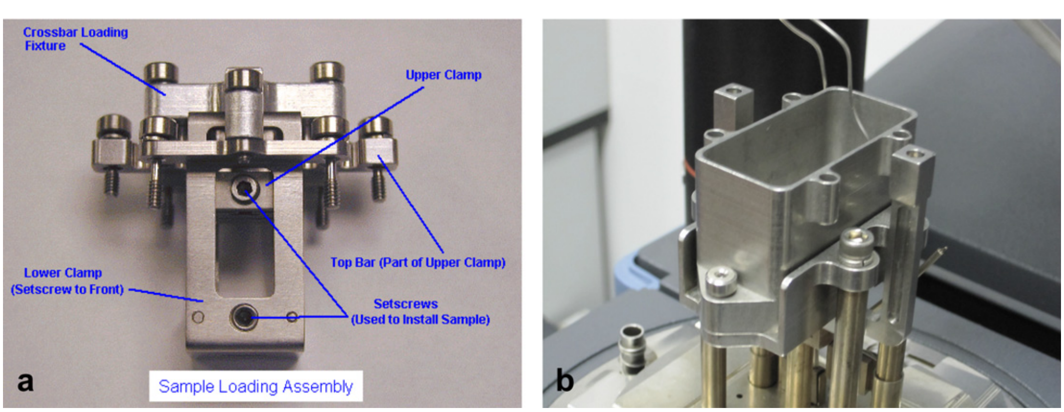


**Fig. 1.** Submersion clamp: (a) the sample loading assembly; (b) the submersion cup.

As reported by Schapery [22] based on thermodynamic analysis, the applied stress levels have little effect on the viscoelastic creep compliance which can be determined using loads in the linear region. The transient creep compliance, $\Delta D(t)$, is typically expressed in the form of a Prony series given in Eq. (4)

$$\Delta D(t) = \sum_{i=1}^{N} D_i\left(1 - \exp^{-t/\tau_i}\right) \tag{4}$$

where $D_i$ are constants and $\tau_i$ are the retardation times. It is better to spread the retardation times uniformly over the logarithmic time scale so as to achieve a good approximation to experimental data, typically with a factor of ten between them. The number of terms ($N$) of the prony series is usually considered to be equal to the number of decades in time over which the equation is used.

For a typical creep-recovery experiment determining the parameters of the nonlinear viscoelastic model as shown in Fig. 2, stress is applied at time $t = 0$ and removed at time $t = t_1$. When the stress input, $\sigma[H(t) - H(t - t_1)]$, is applied, where $H(t)$ is the Heaviside step function, Eq. (1) yield the creep strain

$$\varepsilon_c(t) = g_0 D_0 \sigma_0 + g_1 g_2 \Delta D\left(\frac{t}{a_\sigma}\right)\sigma_0 + \varepsilon_{vp} \quad 0 < t < t_1 \tag{5}$$

and the recovery strain

$$\varepsilon_r(t) = g_2\left[\Delta D\left(\frac{t_1}{a_\sigma} + t - t_1\right) - \Delta D(t - t_1)\right]\sigma_0 + \varepsilon_{vp} \quad t > t_1 \tag{6}$$

Substituting the Prony series representation of creep compliance shown in Eq. (4), the creep strain (Eq. (5)) and recovery strain (Eq. (6)) can be written as [23]

$$\varepsilon_c = D_0 g_0 \sigma_0 + g_1 g_2 \sigma_0 \sum_m D_m\left(1 - \exp\left(-\frac{t}{a_\sigma \tau_m}\right)\right) + \varepsilon_{vp} \quad 0 < t < t_1 \tag{7}$$

$$\varepsilon_r = g_2 \sigma_0 \sum_m D_m\left(1 - \exp\left(-\frac{t_1}{a_\sigma \tau_m}\right)\right)\exp\left(-\frac{t - t_1}{\tau_m}\right) + \varepsilon_{vp} \quad t > t_1 \tag{8}$$

The viscoplastic strain $\varepsilon_{vp}$ accumulated during a loading–unloading cycle can be modeled using the Zapas and Crissman model [24] given as

$$\varepsilon_{vp} = C\left\{\int_o^t [\sigma_T(\tau)]^N \mathrm{d}\tau\right\}^n \tag{9}$$

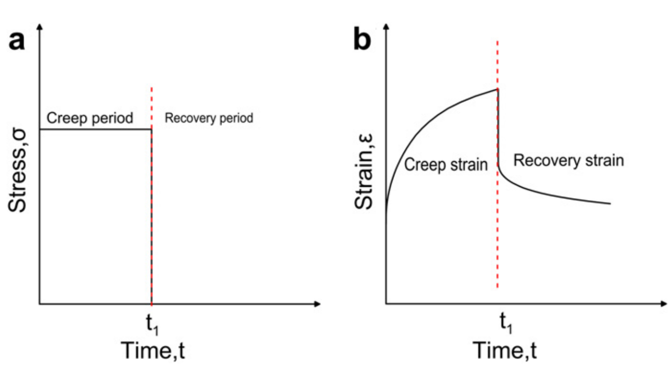


**Fig. 2.** Creep and creep recovery behavior: (a) stress input; (b) strain output for a creep test followed by a recovery period.

When the applied stress is constant with respect to time for a certain period of time, $\sigma_T = \sigma_0$, the viscoplastic strain accumulated during the time interval $t_1$ is as follow

$$\varepsilon_{vp} = C\sigma_0^{N \cdot n} t_1^n \tag{10}$$

The constants $C$, $N$ and $n$ can be determined experimentally by separating the viscoelastic strain and viscoplastic strain from total strains, which involves multiple creep-recovery experiments over single/varying duration and stresses. The experimental method proposed by Nordin and Varna [25] can be described in detail as follows.

In order to determine the stress-dependence of the viscoplastic strains, creep tests of a fixed duration ($t_1$) followed by recovery at several stress levels were carried out. Since viscoelastic strains developed simultaneously with viscoplastic strains, the latter ones cannot be measured directly during operation. Therefore, the irreversible strains obtained at the end of recovery were adopted as an estimation of the total viscoplastic strains developed during respective creep procedure. Plotting the viscoplastic strains versus stress on a log–log scale, the values of '$nN$' and $\log C + n \log t_1$ can be obtained from the plot as the slope of the curve and the $y$-intercept respectively ($\log(\varepsilon_{vp}) = \log C + n \log t_1 + nN \log \sigma$).

Multiple creep tests of durations, $t_1, t_2, \ldots t_r$ on a single specimen at a constant stress $\sigma_0$ were also performed so as to determine the time-dependence of the viscoplastic strains, with each test being followed by a recovery for sufficient time. Assuming that the creep test interruption during the strain recovery period does not affect the plastic strains development (this hypothesis has been validated by many researchers [25,26]), then the viscoplastic strains after $r$ steps of creep loading will be

$$\varepsilon_{vp}^{1+2+\ldots+r} = \varepsilon_{vp}^1 + \varepsilon_{vp}^2 + \ldots \varepsilon_{vp}^r = C\sigma_0^{nN}(t_1 + t_2 + \ldots t_r)^n \tag{11}$$

Similarly, from the curve of the total accumulated viscoplastic strain at the end of each step versus total time on the log–log scale, the exponent '$n$' and $nN \log(\sigma_0) + \log C$ can be estimated as the slope and the $y$-intercept of the curve ($\log(\varepsilon_{vp}) = (nN \log(\sigma_0) + \log C) + n \log t$). Using these values and '$nN$' obtained in previous step, '$N$' and '$C$' can be determined.

## 4. Results and discussion

### 4.1. Determination of onset of nonlinearity

High stress regions resulted from stress concentration sites such as pinholes and cracks are likely to induce nonlinearity in the membrane. Besides, plastic deformation can also lead to the nonlinearity in the membrane stress distribution [6]. The determination of the linear viscoelastic region is one of the most important aspects in the characterization of polymeric materials and their composites. When a viscoelastic material behaves nonlinearly, the isochronous stress–strain curves begin to deviate from linearity at a certain stress level. Hence, isochronous stress–strain plots are needed to identify the stresses which could cause the membrane to behave nonlinearity under immersed condition. As plotted in Fig. 3, the isochronous stress–strain curve shows the increase in the nonlinearity of the stress–strain curve with time, especially at stress higher than 4 MPa. Thus, the strains are nonlinear both with stress and time. It is evident that the stress–strain curves begin to deviate from linearity at the stress of 2 MPa. Therefore, the creep behaviors at the stresses less than 2 MPa can be seen as linearity while that above the region will be defined as nonlinearity. In other words, the stress of 2 MPa is considered approximately to be the borderline of linearity and nonlinearity.

### 4.2. Determination of viscoplastic parameters

To evaluate the viscoplastic Zapas–Crissman parameters, the method proposed by Nordin and Varna [25] which requires only a proportion of data was applied here. Using the method mention in Section 2, the viscoplastic parameters can be obtained. In order to determine the stress-dependence of the membrane, the viscoplastic strains accumulated in the creep tests at the duration of 30 min are plotted against stress on a log–log scale in Fig. 4. Fitting the data in Fig. 4 to a linear function of $X = \log$ (stress) and $Y = \log$ (viscoplastic strain) give the value of $nN = 2.045$ and $\log C + n \log (t_1) = -1.092$ as the slope of the curve and the y-intercept, respectively. Similarly, so as to determine the time-dependence of the membrane, the viscoplastic strains of three durations at the stress of 5 MPa were plotted against time on a log–log scale in Fig. 5. Fitting the data in Fig. 5 to a linear function of $X = \log$ (time), the values of $n = 1.758$ and $nN \log \sigma_0 + \log C = -5.486$ were obtained as the slope and the y-intercept of the curve, respectively. Considering all the values obtained from above procedures, the parameters of the viscoplastic strain can be determined as, $C = 6.8 \times 10^{-8}$, $n = 1.758$, $N = 1.368$.

However in the above procedure for determining the model parameters, two distinctive values for both $n$ and $N$ were obtained by either using $\log C + n \log (t_1)$ from the first curve fit or using $nN \log \sigma_0 + \log C$ from the second curve fit. Through extensively analysis, Dasappa et al. [26] reported that the time-dependence of the viscoplastic strains varies with stress is the main cause. Furthermore, as evidenced by Marklund et al. [23] for tests on flax/polypropylene composites, the power law description of the stress-dependence is rather tough. Therefore, we modify the fitting procedure by splitting the fitting region into two parts: low stress part and high stress part and fitting the experimental data individually as shown in Fig. 4. At lower stress the plastic strain increases with stress much slower than at high stress, thus, two values of $N$ are obtained as

$$N = \begin{cases} 0.664 & \text{for } \sigma < 4\text{ MPa} \\ 3.47 & \text{for } \sigma > 4\text{ MPa} \end{cases}$$

### 4.3. Estimation of nonlinear parameters

The nonlinear viscoelastic constitutive model in Eq. (1) has four nonlinear parameters: $g_0$, $g_1$, $g_2$ and $a_\sigma$. First the Prony coefficients are obtained from creep data using the method of the least square as a 6-term Prony series in the linear viscoelastic region of the material, i.e., at stress level of 1 MPa. The Prony constants and retardation times are given in Table 2.

Once the Prony coefficients are determined, the next step of the analysis will be the mathematical treatment of the experimental data for the estimation of the nonlinear parameters $g_0$, $g_1$, $g_2$ and $a_\sigma$. The most common procedure followed so far, for the estimation of these nonlinear factors, is the curve fitting procedures in the creep and recovery data using numerical analysis method. Since the plastic strains developed in these experiments are relatively small compared to the total creep strains, the instantaneous creep response can be determined directly from the experimental creep curves. Using the following data reduction method proposed by Zaoutsoqa et al. [27,28], the nonlinear parameters can be evaluated. The procedure determining nonlinear parameter included altering $a_\sigma$ in the recovery strain expression and the least square method was then applied to obtain the value of $g_2$ for every value of $a_\sigma$. This procedure

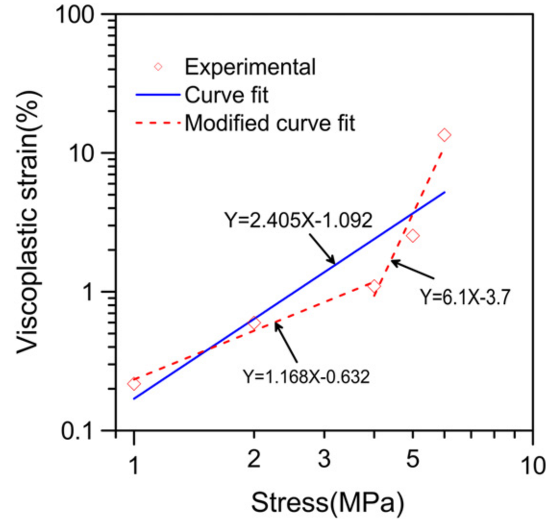


**Fig. 4.** Curve fit of viscoplastic strains at the end of creep–recovery tests for the duration of 30 min on a log–log scale.

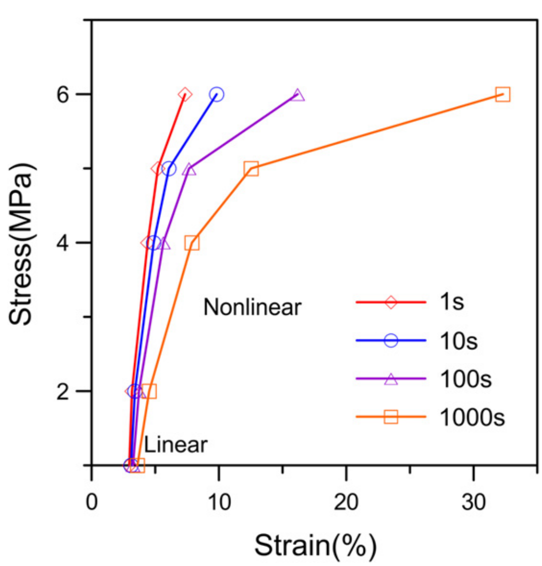


**Fig. 3.** Isochronal stress–strain plot generated from creep tests conducted at different times at 30 °C under immersed condition.

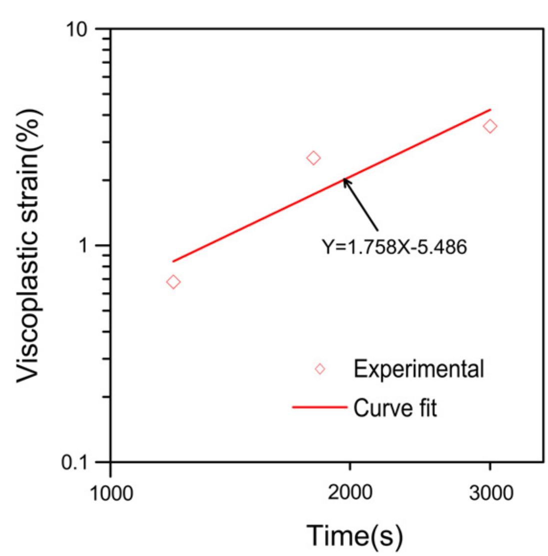


**Fig. 5.** Curve fit of viscoplastic strains at the end of creep–recovery tests at the stress of 5 MPa on a log–log scale at three durations.

**Table 2**
Prony series of linear viscoelastic compliance for $n = 6$ at 30 °C.

| $i$ | $D_i$ ($MPa^{-1}$) | $\tau_i$ (s) |
|---|---|---|
| 1 | 2.33E-04 | 1 |
| 2 | 1.24E-03 | 10 |
| 3 | 3.37E-04 | 50 |
| 4 | 8.98E-04 | 100 |
| 5 | 8.74E-04 | 1000 |
| 6 | 4.50E-03 | 2000 |

continued until a good fitting to experimental data is achieved with the value of $a_\sigma$ and $g_2$ is obtained as well during this procedure. Next, the creep strain is used to determine the other two nonlinear parameters using the least square method with the parameters previously obtained. The creep and creep recovery data and model fit at various stress levels are shown in Fig. 6, from which we can see that the experimental data and model predictions are in well agreement. For clarity, we separate the stress levels into two parts, since strains at stresses higher than 4 MPa were much larger, making it hard to recognize for stains at lower stresses when put into one picture.

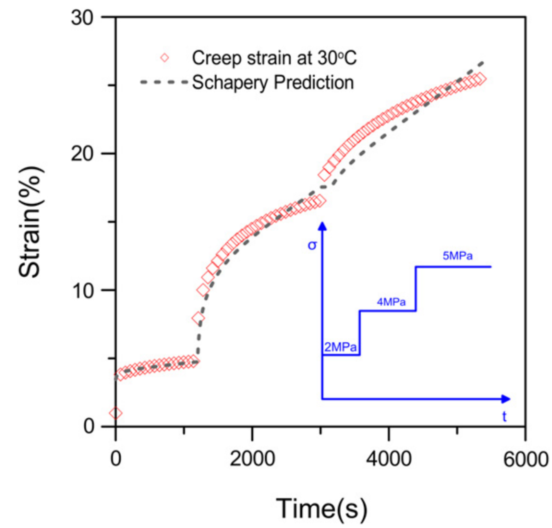


**Fig. 7.** Nonlinear viscoelastic Schapery model validation for step-stress profiles.

### 4.4. Validation of the model

To validate the nonlinear model, a step-stress input profile is used at 30 °C as can be seen in the bottom of Fig. 7, with the membrane creep at 2 MPa for 20 min followed by creep at 4 MPa for 30 min and then creep at 5 MPa for 40 min. From the figure, it can be observed that the experimental results have fair agreement with the predicted values except for data in the third step. In general, to some extent, this result can validate the nonlinear model and meanwhile account for the nonlinear viscoelastic–plastic behavior of the membrane.

### 4.5. Modification of the model

However, when it comes to describe the creep behavior of the membrane at temperature of 70 °C with the method described in previous section (dash line), the results are far less satisfactory as shown in Fig. 8. Differences of the behaviors of the membrane at two temperatures lies in that the creep curve soon reaches equilibrium after a certain period of time at 70 °C, while at 30 °C the creep strains keep increasing and has no tendency of equilibrium within limited time. This phenomenon might be attributed to the stiffening effect of the PEM in liquid water at certain high temperature, which was also observed by Bauer et al. [13]. In this case, the previously described model (referred as unmodified model in the following) is not able to capture the trend when the creep strain reached a plateau, since the creep strain would keep increasing with time when simulated by the unmodified model. According to the expression of creep strain in Eq. (7), both the plastic and elastic components contribute to the differences between experimental data and prediction values. In the elastic component, the time in exponent form can greatly influence the time to reach a plateau, therefore, a modified factor, $n$, is introduced to account for the time acceleration effect. The modified form of Eq. (7) can be expressed as:

$$\varepsilon_c = D_0 g_0 \sigma_0 + g_1 g_2 \sigma_0 \sum_m D_m \left(1 - \exp\left(-\frac{t^n}{a_\sigma \tau_m}\right)\right) + \varepsilon_{vp} \quad 0 < t < t_1 \tag{12}$$

By fitting of the creep data of 3 MPa at 70 °C, $n$ could be obtained and the modified curve (dash dot line) is shown in Fig. 9. Although the distinction between the prediction value and experimental data is minor, the modified equation still cannot characterize the creep behavior for the increasing plastic strain with time. Hence, the viscoplastic strain is modified as:

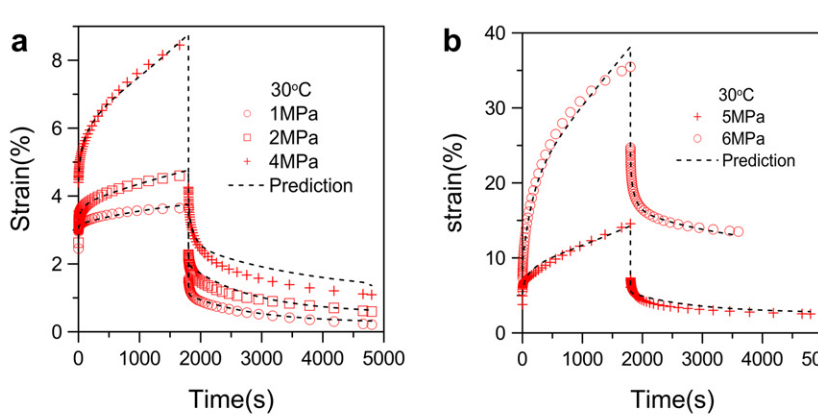


**Fig. 6.** Creep and creep recovery data and model fit at various stress levels: (a) $\sigma \le 4$ MPa; (b) $\sigma > 4$ MPa.

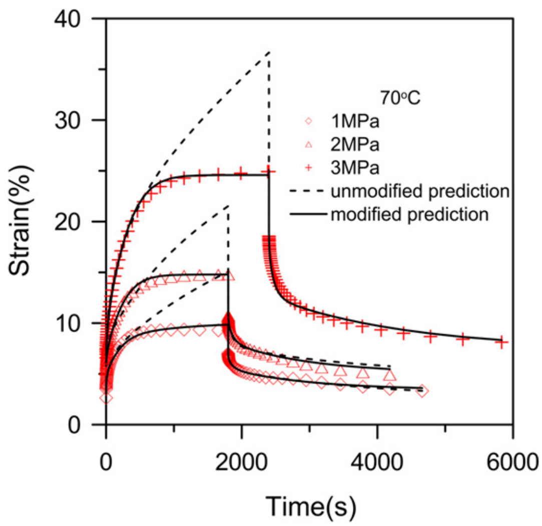


**Fig. 8.** Comparison of experimental data (1 MPa, 2 MPa and 3 MPa) and prediction values of both unmodified and modified model at 70 °C.

$$\varepsilon_{vp} = A\ln\left(1-\frac{\sigma_0}{Q}\right)[1-\exp(-bt)] \tag{13}$$

Similarly, the constants $A$, $Q$ and $b$ can be determined using data obtained from creep–recovery experiments over single/varying duration and stresses. Particularly, at a fixed stress, creep tests data of different durations are used to obtain the constant $b$ and $A\ln(1-\sigma_0/Q)$. Likewise, $Q$ and $A[1-\exp(-bt)]$ can also be obtained with data from creep tests of varying stresses at a constant duration. The constant $A$ can be got either from $A\ln(1-\sigma_0/Q)$ or $A[1-\exp(-bt)]$ and theoretically these two expressions will yield identical value of $A$. Prediction values (solid line) after modification of both the elastic and plastic components are in well agreement with experimental ones as shown in Fig. 9. In this way, prediction values of the modified model at different stresses are also obtained and presented in Fig. 8 (solid line).

The modified model is also used to describe the creep–recovery behavior of the membrane at 30 °C to validate its universality as

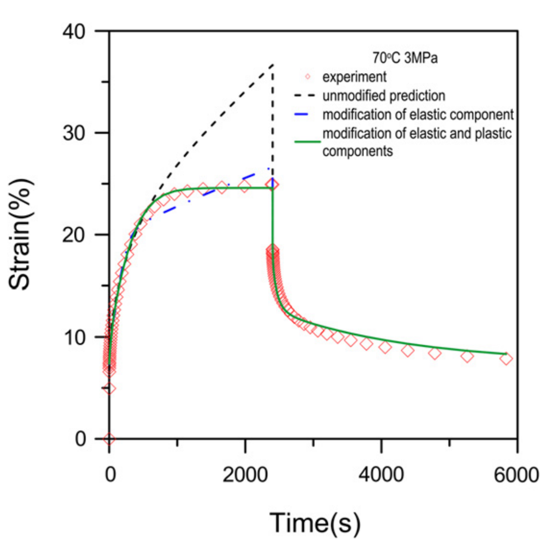


**Fig. 9.** Comparison of experimental data (3 MPa) and different model prediction values at 70 °C.

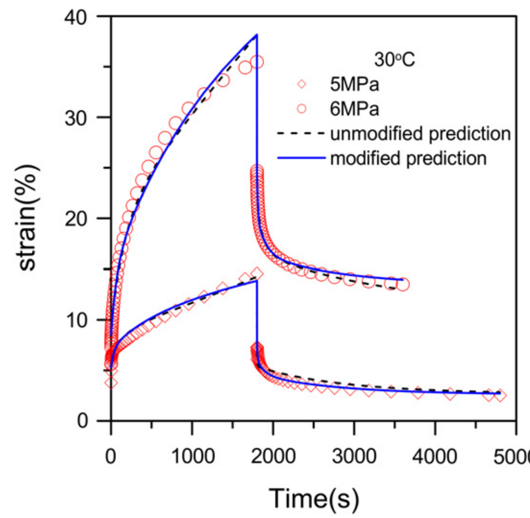


**Fig. 10.** Comparison of experimental data (5 MPa and 6 MPa) and prediction values of both unmodified and modified model at 30 °C.

shown in Fig. 10. Obviously, pretty good agreement is achieved between prediction values of the modified model and experimental data. It shows that the modified model can characterize the actual strain revolution of the membrane within the temperature range of our study.

## 5. Conclusion

A nonlinear viscoelastic–plastic constitutive model is used to characterize the behaviors of PEMs under submersion condition based on the general nonlinear constitutive relation given by Schapery and the nonlinear parameters are determined by fitting creep–recovery test data. The nonlinearity of the membrane is determined by constructing isochronal stress–strain curves and the time-dependent behavior of the material is observed. Furthermore, the stress-dependent and time-dependent of the viscoplastic strains are determined using method proposed by Nordin through measuring the irreversible strains after creep tests of different creep durations at the same stress and creep tests of a fixed duration but at different stresses. With the data reduction method reported by Zaoutsoqa, all the nonlinear parameters are obtained. The experimental data are found to agree quite well with the fitting values at various stresses and durations. A step-stress test for validation of the model is conducted at 30 °C and reasonable agreement is achieved between experimental and prediction values. The creep–recovery curves at 70 °C are quite different from that at 30 °C and a modified model is proposed to capture this distinction. Prediction values at both 30 °C and 70 °C are in fair agreement with the experimental ones.


## Acknowledgement

The authors gratefully acknowledge financial support for this work from the Program of Introducing Talents of Discipline to Universities (No: B06006). Partial support (No. 2011NGQ003) from Key Laboratory of Efficient & Clean Energy Utilization, College of Hunan Province, is acknowledged.


## References


[1] A. Kusoglu, Y.L. Tang, M. Lugo, A.M. Karlsson, M.H. Santare, S. Cleghorn, W.B. Johnson, J. Power Sources 195 (2010) 483–492.

[2] A. Kusoglu, A.M. Karlsson, M.H. Santare, S. Cleghorn, W.B. Johnson, J. Power Sources 161 (2006) 987–996.
[3] M. Marrony, R. Barrera, S. Quenet, S. Ginocchio, L. Montelatici, A. Aslanides, J. Power Sources 182 (2008) 469–475.
[4] A. Kusoglu, A.M. Karlsson, M.H. Santare, S. Cleghorn, W.B. Johnson, J. Power Sources 170 (2007) 345–358.
[5] K.A. Patankar, D.A. Dillard, S.W. Case, M.W. Ellis, Y.H. Lai, M.K. Budinski, C.S. Gittleman, Mech. Time-Depend. Mater. 12 (2008) 221–236.
[6] M.N. Silberstein, M.C. Boyce, J. Power Sources 196 (2011) 3452–3460.
[7] W. Yoon, X. Huang, J. Power Sources 196 (2011) 3933–3941.
[8] R. Solasi, Y. Zou, X. Huang, K. Reifsnider, D. Condit, J. Power Sources 167 (2007) 366–377.
[9] P.W. Majsztrik, A.B. Bocarsly, J.B. Benziger, Macromolecules 41 (2008) 9849–9862.
[10] S. Kundu, L.C. Simon, M. Fowler, S. Grot, Polymer 46 (2005) 11707–11715.
[11] X.Y. Huang, R. Solasi, Y. Zou, M. Feshler, K. Reifsnider, D. Condit, S. Burlatsky, T. Madden, J. Polym. Sci. Part B Polym. Phys. 44 (2006) 2346–2357.
[12] R. Solasi, Y. Zou, X. Huang, K. Reifsnider, Mech. Time-Depend. Mater. 12 (2008) 15–30.
[13] F. Bauer, S. Denneler, M. Willert-Porada, J. Polym. Sci. Part B Polym. Phys. 43 (2005) 786–795.
[14] C.M. Gates, J. Newman, AIChE J. 46 (2000) 2076–2085.
[15] P. Choi, R. Datta, J. Electrochem. Soc. 150 (2003) E601–E607.
[16] A.Z. Weber, J. Newman, J. Electrochem. Soc. 150 (2003) A1008–A1015.
[17] K.A. Mauritz, R.B. Moore, Chem. Rev. 104 (2004) 4535–4585.
[18] L.M. Onishi, J.M. Prausnitz, J. Newman, J. Phys. Chem. B 111 (2007) 10166–10173.
[19] M. Bass, A. Berman, A. Singh, O. Konovalov, V. Freger, J. Phys. Chem. B 114 (2010) 3784–3790.
[20] Y. Lou, R.A. Schapery, J. Compos. Mater. 5 (1971) 208–234.
[21] R.A. Schapery, A.F.M.L. Research, T. Division, Further Development of a Thermodynamic Constitutive Theory: Stress Formulation Report AA & ES 69-2, Purdue University, Lafayette, Ind, 1969.
[22] R.A. Schapery, Mech. Time-Depend. Mater. 1 (1997) 209–240.
[23] E. Marklund, J. Varna, L. Wallström, J. Eng. Mater. Technol. 128 (2006) 527–536.
[24] L. Zapas, J. Crissman, Polymer 25 (1984) 57–62.
[25] L.O. Nordin, J. Varna, Compos. Part A Appl. Sci. Manuf. 37 (2006) 344–355.
[26] P. Dasappa, P. Lee-Sullivan, X. Xiao, Compos. Part B Eng. 41 (2010) 48–57.
[27] S. Zaoutsos, G. Papanicolaou, A. Cardon, Compos. Sci. Technol. 58 (1998) 883–889.
[28] G. Papanicolaou, S. Zaoutsos, A. Cardon, Compos. Part A Appl. Sci. Manuf. 30 (1999) 839–848.